

Abstract

AGN Jets are observed to possess various sites for particle acceleration, which gives rise to the observed non-thermal spectra. Diffusive shock acceleration (DSA) and stochastic turbulent acceleration (SA) are claimed to be the candidates for producing very high energetic particles in weakly magnetized regions. While DSA is a systematic acceleration process, SA is a random energization process, which is usually modelled as a biased random walk in energy space with a Fokker-Planck equation. Due to the ubiquitous nature of plasma fluctuations, SA gives rise to diffuse emission, whereas DSA leads to localized emission. In astrophysical systems, different acceleration processes work in an integrated manner along with various energy losses. I will present our novel method of implementing SA in the hybrid Eulerian-Lagrangian framework that accounts for DSA in the presence of radiative processes like synchrotron and IC emission. The focus would be to showcase the interplay between the particle acceleration process due to shocks and turbulence. Further, I will also discuss the application of these acceleration mechanisms in governing the characteristic of the non-thermal emission from AGN jets.

Motivation

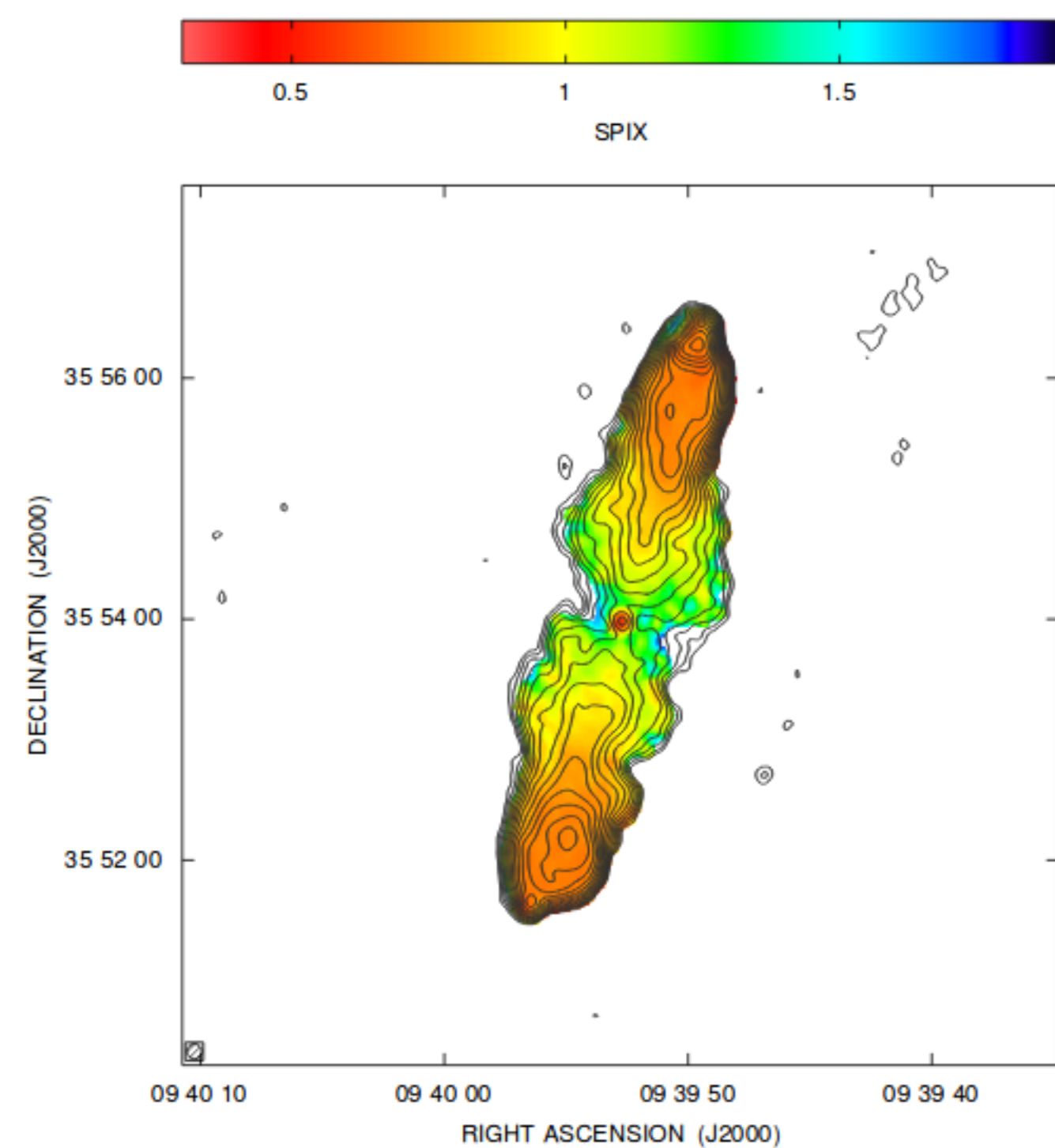


Figure: Spectral index map between 327 MHz and 1.48 GHz of 3C223, radio galaxy, taken by VLA plotted with 327 MHz Radio Contours. [Orrù & et al., 2010]

- ▶ Simulating the spectral maps for AGN radio lobes and Galaxy Cluster relics.
- ▶ Comparison between spectral age and dynamical age for these structures.
- ▶ Competition and complementary actions between various particle acceleration mechanisms.

Modelling Fermi IInd order

$$\frac{\partial \chi_p(\gamma, \tau)}{\partial \tau} = \frac{\partial}{\partial \gamma} \left\{ - [S(\gamma, \tau) + D_A(\gamma, \tau)] \chi_p(\gamma, \tau) + D_{\gamma\gamma}(\gamma, \tau) \frac{\partial \chi_p(\gamma, \tau)}{\partial \gamma} \right\} - \frac{\chi_p}{T_{\text{esc}}} + Q. \quad - [Webb (1989)]$$

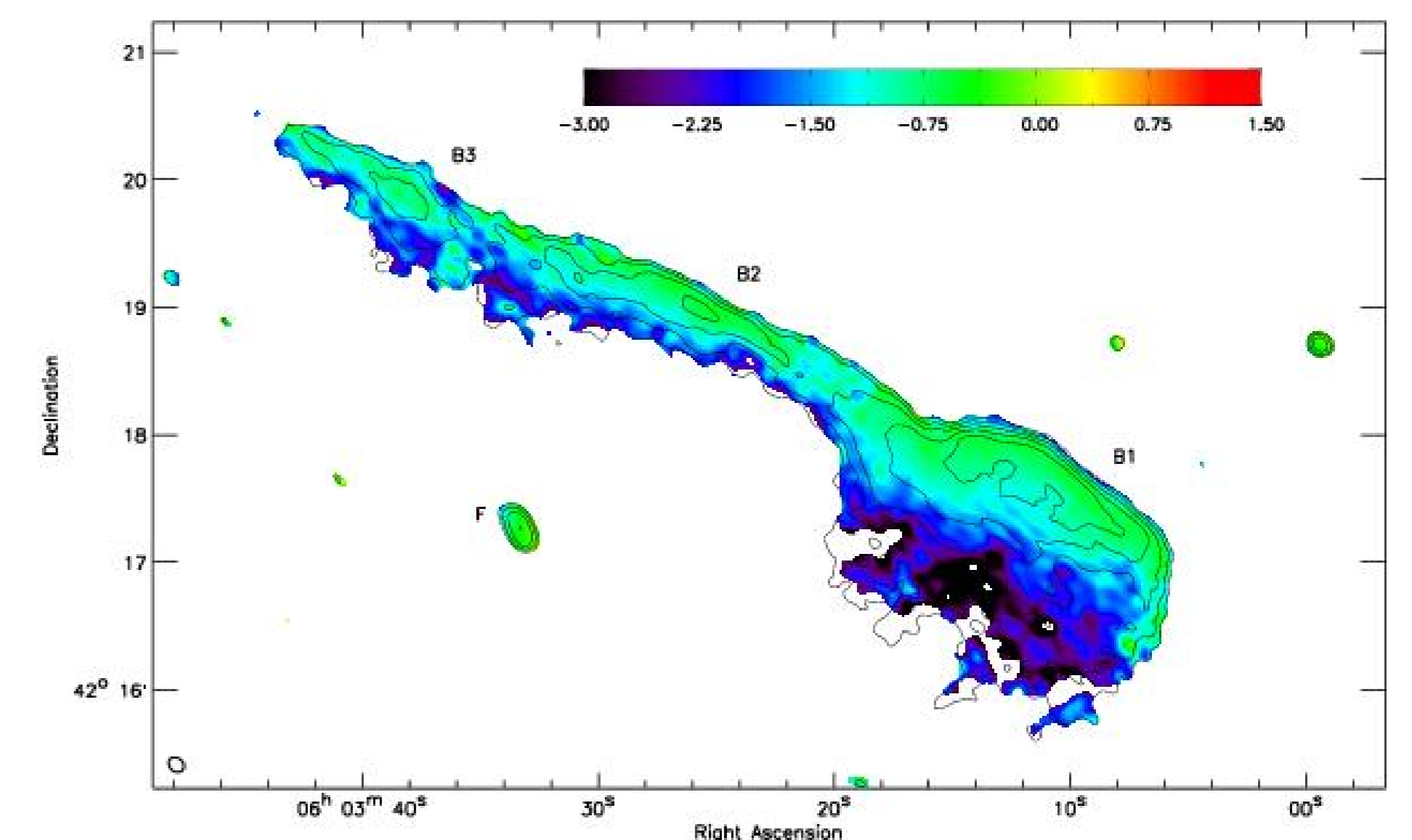


Figure: Spectral index map between 325 MHz and 610 MHz of toothbrush cluster's radio relic, radio galaxy, taken by GMRT plotted with 325 MHz Radio Contours. [van Weeren et al., 2016]

Numerical Implementation of Stochastic Acceleration

Analytical Validation with Hard Sphere Equation (Park & Petrosian, 1995)

$$\frac{\partial \chi_p}{\partial \tau} = \frac{\partial}{\partial \gamma} \left(\gamma^2 \frac{\partial \chi_p}{\partial \gamma} - \gamma \chi_p(\gamma, \tau) \right) - \chi_p; \quad \chi_p^{\tau=0} = \frac{e^{-1.0}}{\gamma \sqrt{4\pi}} \exp \left(- \frac{[\log(\frac{100}{\gamma}) + 2]^2}{4} \right).$$

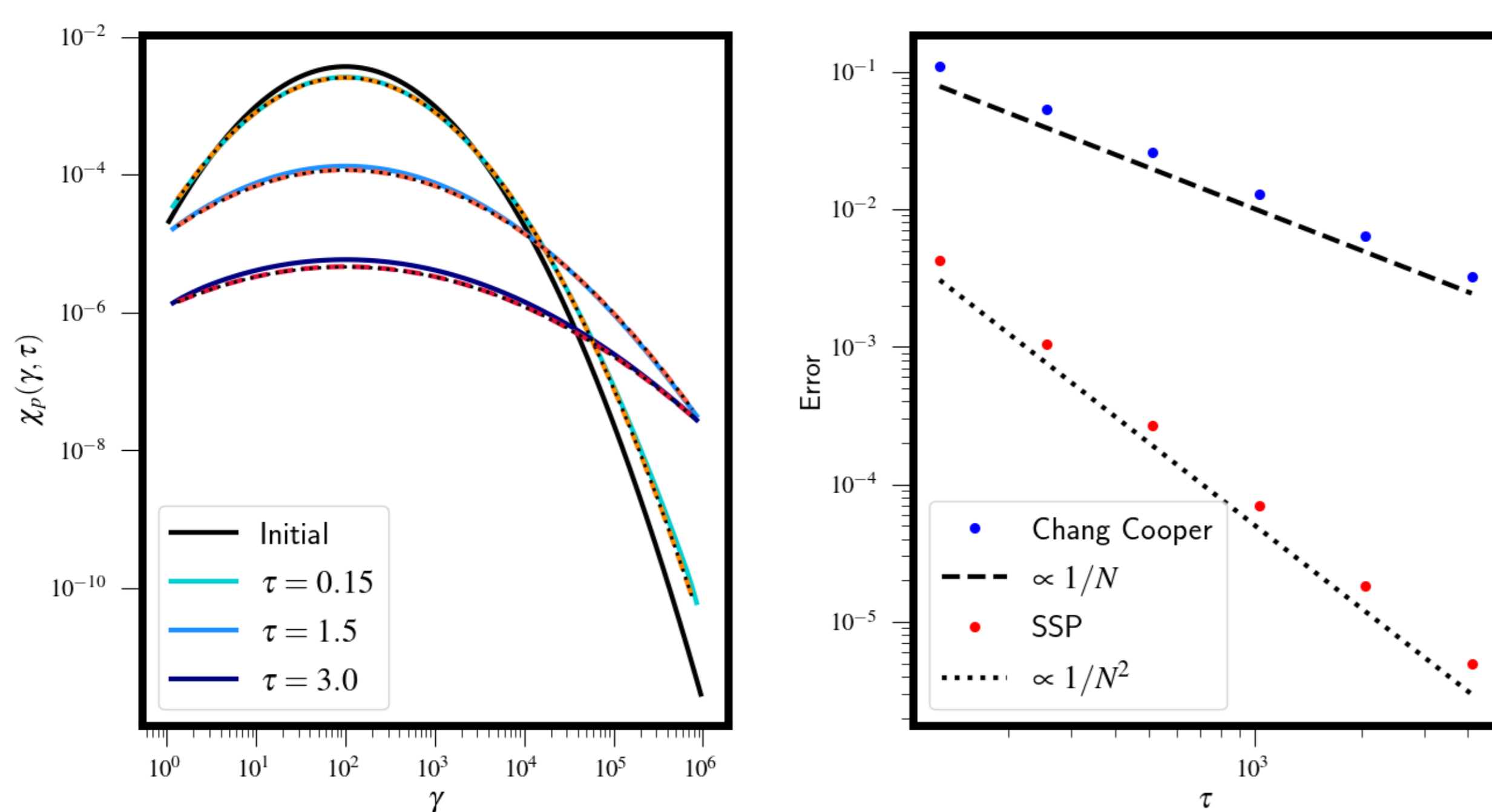


Figure: **Left:** Evolution of χ_p for both the schemes SSP and Chang Cooper at different times (τ). **Blue Solids** due to Chang Cooper scheme, **Red dashed** due to SSP and **Black dots** are due to analytical. **Right:** L_1 error convergence for both the schemes.

Planar Shock: Interplay of Shock and turbulent acceleration

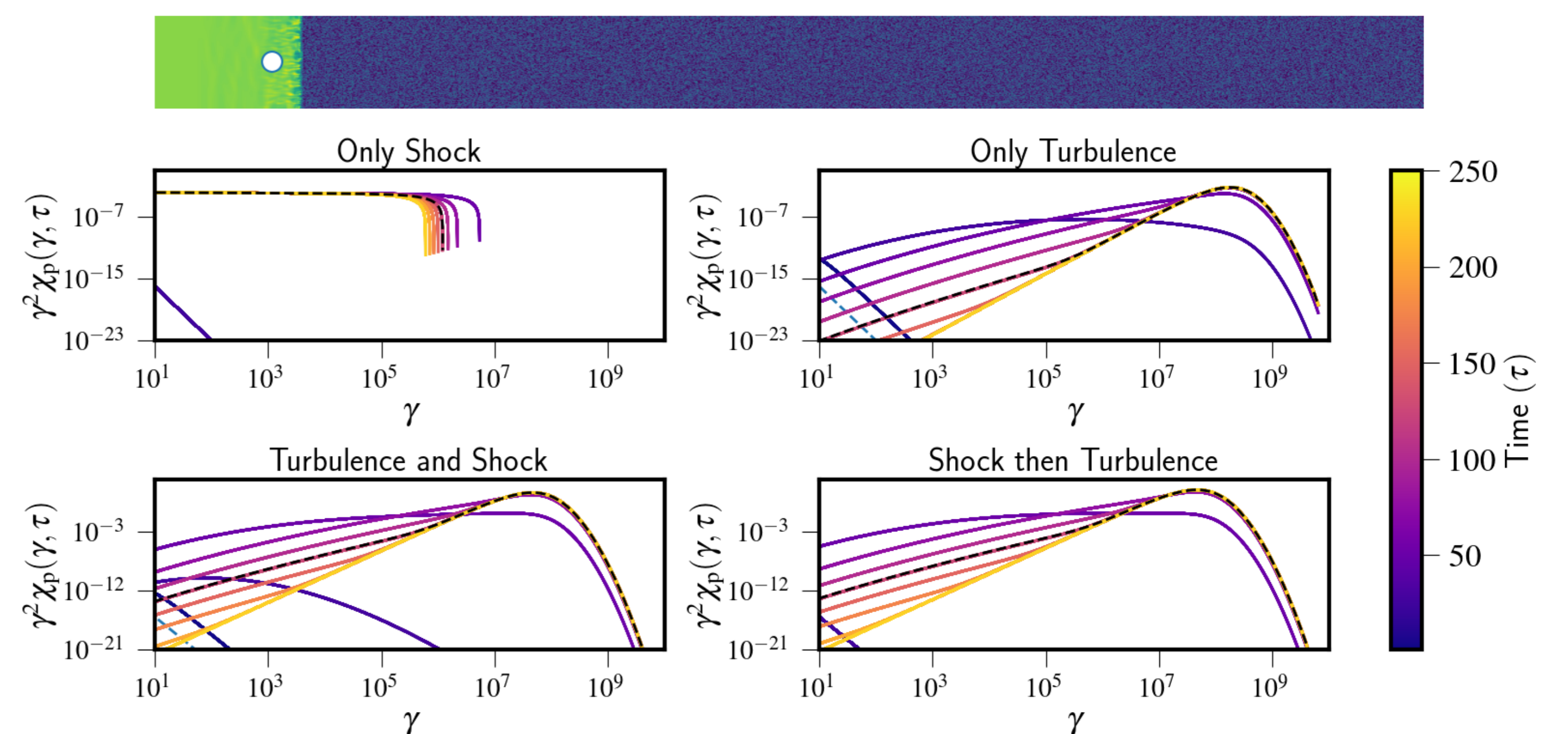


Figure: **Top section:** Density map of a fluid where a particle (shown in white dot) initially located at $(x, y) \equiv (1.5, 0.0)$, moves with the fluid and crosses shock. The upstream region is shown in blue and the downstream region is shown in green. **Lower section:** Evolution of $\gamma^2 \chi_p$ for different acceleration scenarios, $D_{\gamma,\gamma} \propto \gamma^2$ and synchrotron, IC and adiabatic losses. The compression ratio of the shock is taken to be 3.86. The black dashed curve shows the particle energy spectrum for the same time when the density map snapshot is taken.

Simulated emission from AGN Jet: Effect of turbulent and shock acceleration

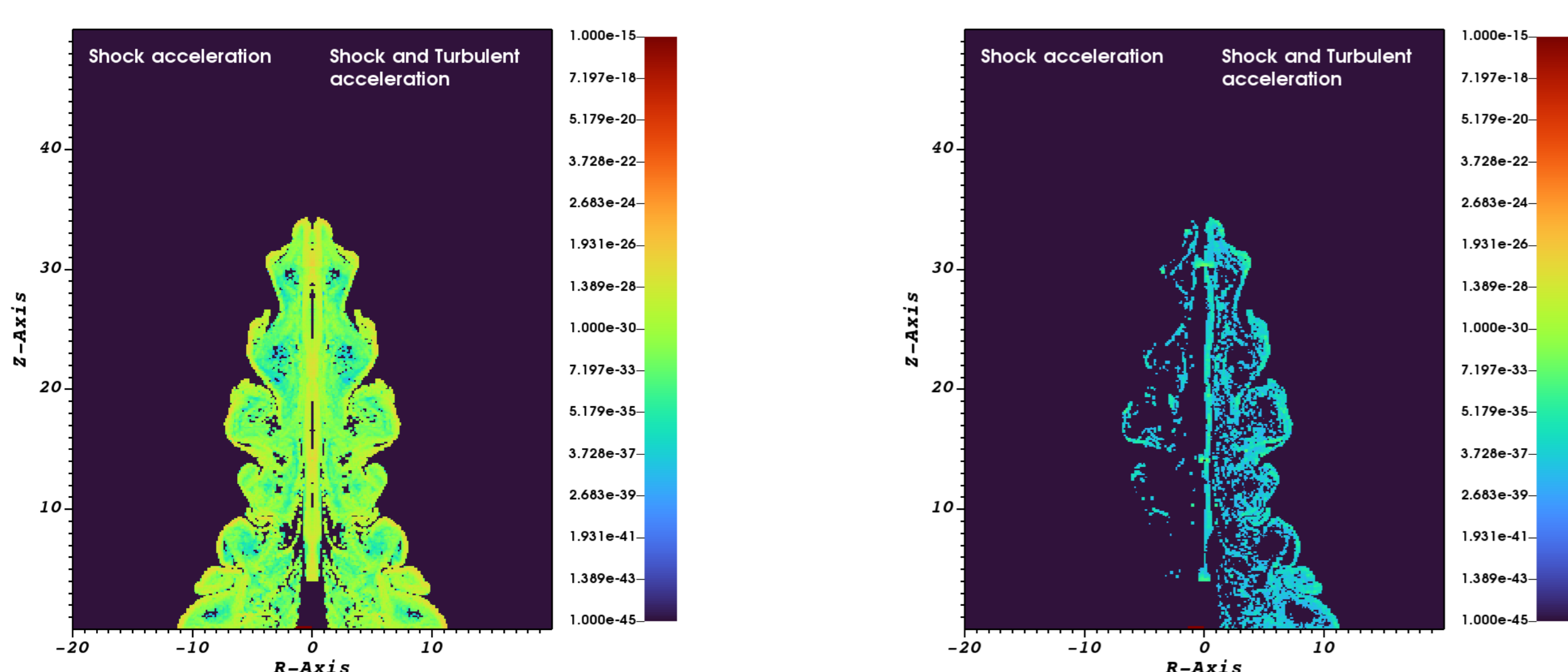


Figure: Comparison between the emission from turbulence and shock acceleration and only shock acceleration for radio frequency, 1.4 GHz.

Figure: Comparison between the emission from turbulence and shock acceleration and only shock acceleration for 0.4 KeV X-Ray.

AGN Jet simulation is done following Mignone et al. (2009). The particle spectrum is calculated following Eq. (1) (for turbulent case) and following Vaidya et al. (2018) (for the shock case).

Conclusions

- ▶ Our algorithm gives an order of magnitude higher accuracy than all the existing codes on a non-uniform log grid, for full Fokker-Planck equation (here we consider Chang Cooper also see Winner et al. (2019)).
- ▶ Module is incorporated, as an extension to the lagrangian module (Vaidya et al., 2018), in PLUTO (Mignone et al., 2007) and applied to various test problems.
- ▶ Showcasing the competing and complementing actions of various acceleration processes.
- ▶ Due to turbulent acceleration with shock we obtain significant emission signatures at very high frequency (0.4 KeV X-Ray) which could not be seen if only shock acceleration is taken into account.

References

- Mignone A., et al., 2007, The Astrophysical Journal Supplement Series, 170, 228
Mignone A., Ugliano M., Bodo G., 2009, Monthly Notices of the Royal Astronomical Society, 393, 1141
Orrù E., et al. 2010, A&A, 515, A50
Park B. T., Petrosian V., 1995, ApJ, 446, 699
Vaidya B., Mignone A., Bodo G., Rossi P., Massaglia S., 2018, The Astrophysical Journal, 865, 144
Webb G. M., 1989, ApJ, 340, 1112
Winner G., Pfrommer C., Girichidis P., Pakmor R., 2019, Monthly Notices of the Royal Astronomical Society, 488, 2235
van Weeren R. J., et al., 2016, The Astrophysical Journal, 818, 204